

Modeling controlled propagation of molecular polarization induced by wave-packet dynamics

J. D. Lee¹ and J. Inoue^{1,2}

¹International Center for Young Scientists, National Institute for Materials Science, Tsukuba 305-0044, Japan

²Nanomaterials Laboratory, National Institute for Materials Science, Tsukuba 305-0044, Japan

(Received 15 November 2005; published 6 April 2006)

We study the propagation of molecular polarization induced by a local excitation and its motion on the one-dimensional molecular array adsorbed on the host material. The local excitation can be either an electron wave packet or an exciton in a given molecular complex. It is found that there exist three different kinds of propagation of molecular polarization—two kinds of ballistic propagation and one diffusive propagation—depending on the values of ω_0/t and g/t , where ω_0 is the excitation energy of polarization, t the electron (or exciton) hopping, and g the coupling between electron and polarization. Ballistic propagation can be understood as a bare electron's motion, while diffusive propagation implies the formation of a massive polaron. In a realistic situation, a propagating electron can be captured with a finite probability via tunneling through the adlayer energy barrier into the host material. Such effects of tunneling on the polarization propagation are investigated to examine the possibilities or limitations for controlling an array of polarization. Finally, we discuss the recent implementation of the scanning tunneling microscope (STM)-induced polarization of functional molecular nanostructures within our framework.

DOI: [10.1103/PhysRevB.73.165404](https://doi.org/10.1103/PhysRevB.73.165404)

PACS number(s): 68.35.Ja, 71.35.Aa, 71.38.-k, 78.47.+p

I. INTRODUCTION

The physics of excess electrons (or elementary excitations like excitons) at interfaces is not only of fundamental importance, but also of renewed interest due to its potential for application to nanoscale fabrication, molecular electronics, and electrochemistry. The origin of excess electrons can be either photoemission from lower occupied states,¹⁻³ or electron-injection by external perturbations such as a short optical pulse⁴⁻⁶ or a scanning tunneling microscope (STM).^{7,8} In the former case, excess electrons exist in the delocalized states, but in the latter case, electrons initially exist in the wave packets. Such electrons at the interface of molecular adlayers on metal/semiconductor substrates propagate and interact with molecules. Electrons drag or move in a bound state with polarization (“*polaron*”) and accompany propagation of polarization in condensed media. In this way, an interaction between electrons and molecules decides the fate of each other in the ultrafast time region, i.e., within $\mathcal{O}(1)$ ps.

Recently, many experiments have been conducted for the time-resolved observation of physical phenomena using the so-called *pump-probe spectroscopy*, reinterpreting the results in terms of the fundamental time scales of electronic or nuclear motion.^{9,10} Within the experimental framework, the questions of how a bare electron becomes a polaron or how long it takes for the polaron to form have been explored.^{1,2} In those studies, it has been observed that delocalized bare electrons self-trap as small polarons within 1 ps in strongly coupled electron-phonon systems. The dynamics of localized electron states (wave packets) have also been investigated through an interplay between their electronic and vibrational degrees of freedom in the quasi-one-dimensional system ([Pt(en)₂][Pt(en)₂I₂](ClO₄)₄; en=ethylenediamine) using time-resolved spectroscopy.^{4,5} In another respect, the polaron propagation can be also used for controlling nanoscale fab-

rication by reorganizing molecules surrounding an electron to accommodate the electron's charge density.^{7,8} Okawa and Aono⁷ have induced a linear chain chemical reaction on the monomolecular layer of diacetylene compounds using STM. The reaction occurs spontaneously after being initiated by a STM tip, not by continuous scanning. A STM tip stimulates a local chemical reaction on the molecular layer.¹¹ Such a chemical reaction can be understood to originate a local molecular modification on the layer, which can be formally (in the mathematical treatment) regarded as an exciton (i.e., Frenkel exciton) that propagates and induces the molecular chain reaction. It is then an interesting problem to understand the dynamics of molecules triggered by an injection of a local excitation in such a short time span where an entire process occurs.

We propose a model of a local excitation and molecules in one-dimensional (1D) molecular array on a substrate matrix. The local excitation can be either an electron wave packet or an exciton injected by the external perturbation. The dynamics of the system are started by the sudden creation of an electron (or *exciton without any loss of validity in the whole scope of the present work*) by an external manipulation at the designated position on the array. The electron then moves on the molecular sites and induces local molecular polarizations. Molecular polarizations can be local phonons, local electronic excitations, or other relevant molecular excitations depending on the system under consideration. There is a large body of works to describe those switching phenomena, most of which have concentrated on finding the metastable states hidden in equilibrium by approaches analogous to those in thermodynamics.¹² As a matter of fact, such works cannot describe true dynamical features of the system, especially at the very early stage (at the stage showing transient behaviors before equilibrium, i.e., in the ultrafast time region) after switching on the external manipulation or perturbation. In this paper, however, we investigate the dynamics of an electron and molecules, and the spontaneous occur-

rence and propagation of molecular polarization in the ultrafast time region using many-body time-dependent diagonalization (MTD). The time-evolution of a whole many-body system within the many-body Hilbert space is explored by solving the time-dependent Schrödinger equation.¹³⁻¹⁵ An excess electron would be finally captured by tunneling through an energy barrier into the substrate. Such tunneling can be also accounted for in the dynamics by including the substrate states in the many-body Hilbert space. In this study, we address the following questions: (i) How does the molecular polarization propagate in the femtosecond or picosecond region after an electron-injection? (ii) Are there any qualitatively different types of propagation depending on electronic or molecular degrees of freedom? (iii) How can we control such propagation?

The paper is organized as follows. In Sec. II, we give a model of the system and describe the formalism to follow. In Sec. III, the propagation of molecular polarization is studied in detail. In the section, we find a phase diagram of three different types of propagation depending on the parameters of the system and elucidate the physical properties of each type of propagation. In Sec. IV, we consider the capture of an electron through tunneling into a substrate and its effects on the propagation of polarization, which could better simulate realistic situations. Finally, in Sec. V, we discuss a realistic system to which the present model can be practically applied and provide a summary and conclusion.

II. MODEL AND FORMALISM

We take the local excitation as an injected “electron” wave packet hereafter unless stated otherwise; it does not lose any validity or applicability. The dynamics of an electron and molecules on the 1D molecular array can then be described by the following Hamiltonian

$$\begin{aligned} \mathcal{H} = & t \sum_i (c_i^\dagger c_{i+1} + c_{i+1}^\dagger c_i) + \frac{\omega_0}{2} \sum_i (1 + \sigma_i) + g \sum_i c_i^\dagger c_i (\sigma_{i+} \\ & + \sigma_{i-}) + \sum_i \int d\varepsilon T(\varepsilon) (c_i^\dagger \psi_\varepsilon + \psi_\varepsilon^\dagger c_i) + \int d\varepsilon \varepsilon \psi_\varepsilon^\dagger \psi_\varepsilon. \end{aligned} \quad (1)$$

$c_i^\dagger(c_i)$ is the electron operator at site i and t is the electron hopping. ω_0 is the excitation energy of the molecular polarization. The molecular energy structure is assumed not to be affected by its polarization state. g is a coupling constant between electron and molecular polarization. An excitation of local molecular polarization at site i can be treated as a bosonic operator b_i^\dagger . Assuming only a single excitation per site (i.e., only the fundamental excitation of $|\text{vac}\rangle \rightarrow b_i^\dagger |\text{vac}\rangle$ excluding higher order polarized states like $(b_i^\dagger)^n |\text{vac}\rangle$ with $n > 1$, where $|\text{vac}\rangle$ is the vacuum state), each molecule has two levels and a molecular array can then be approximated as an array of pseudospins of $S=1/2$, i.e., $b_i^\dagger = \frac{1}{2} \sigma_{i+}$, $b_i = \frac{1}{2} \sigma_{i-}$, and $b_i^\dagger b_i = \frac{1}{2} (1 + \sigma_i)$,¹⁶ where σ_{i+} , σ_{i-} , and σ_i are Pauli matrices. Now in the spin system, a molecular polarization is described by a pseudospin flip. $\psi_\varepsilon^\dagger(\psi_\varepsilon)$ is the operator of the substrate electron with its continuum energy ε . With the tun-

neling matrix $T(\varepsilon)$, the electron on the molecular array can be captured into the substrate.

An electron-injection in the form of a wave packet can be treated as an approximation of the sudden existence of an electron at the desired position on the molecular array. The necessary Hilbert space then consists of an electron on the array, pseudospins, and a substrate electron. The state of a whole system within the many-body Hilbert space can be expressed as

$$\begin{aligned} |\Psi(\tau)\rangle = & \sum_i \sum_{\{\sigma\}} C_{i\{\sigma\}}(\tau) |i\rangle |0\rangle_\varepsilon |\{\sigma\}\rangle \\ & + \sum_{\{\sigma\}} \int d\varepsilon C_{\varepsilon\{\sigma\}}(\tau) |O\rangle |\varepsilon\rangle |\{\sigma\}\rangle. \end{aligned} \quad (2)$$

The state of an electron at the molecular site i is $|i\rangle = |0\rangle |0\rangle \cdots |1\rangle_{i\text{th}} \cdots |0\rangle |0\rangle$ and the state without an electron on the molecular array is $|O\rangle = |0\rangle |0\rangle \cdots |0\rangle |0\rangle$, while that of pseudospins (molecules, i.e., molecular polarizations) can be written as a product of each spin's, i.e., $|\{\sigma\}\rangle = \prod_i |\sigma_i\rangle$. $|\varepsilon\rangle$ is the continuum state of a substrate electron with its energy ε and $|0\rangle_\varepsilon$ is the substrate state without an electron. Dynamics which start by an electron-injection can be described by solving the time-dependent Schrödinger equation $i\partial/\partial\tau |\Psi(\tau)\rangle = \mathcal{H} |\Psi(\tau)\rangle$ with $|\Psi(0)\rangle = |i_0\rangle |0\rangle_\varepsilon |\{\sigma\}_0\rangle$, where i_0 is the designated position for an electron-injection and the initial state for pseudospins is $|\{\sigma\}_0\rangle = |-\rangle |-\rangle \cdots |-\rangle |-\rangle$ at zero temperature or low temperatures compared to ω_0 . This is the basic scheme of MTD.^{14,15}

The time-dependent Schrödinger equation gives coupled differential equations for $C_{i\{\sigma\}}(\tau)$ and $C_{\varepsilon\{\sigma\}}(\tau)$,

$$\begin{aligned} i \frac{\partial}{\partial \tau} C_{i\{\sigma\}}(\tau) = & t C_{i+1\{\sigma\}}(\tau) + t C_{i-1\{\sigma\}}(\tau) \\ & + \frac{\omega_0}{2} \left[\sum_{\sigma_l \in \{\sigma\}} (1 + \sigma_l) \right] C_{i\{\sigma\}}(\tau) \\ & + g C_{i\{\sigma; \sigma_i \rightarrow -\sigma_i\}}(\tau) + \int d\varepsilon T(\varepsilon) C_{\varepsilon\{\sigma\}}(\tau), \end{aligned} \quad (3)$$

$$\begin{aligned} i \frac{\partial}{\partial \tau} C_{\varepsilon\{\sigma\}}(\tau) = & \frac{\omega_0}{2} \left[\sum_{\sigma_l \in \{\sigma\}} (1 + \sigma_l) \right] C_{\varepsilon\{\sigma\}}(\tau) + T(\varepsilon) \sum_i C_{i\{\sigma\}}(\tau) \\ & + \varepsilon C_{\varepsilon\{\sigma\}}(\tau), \end{aligned} \quad (4)$$

where $\{\sigma; \sigma_i \rightarrow -\sigma_i\}$ means a configuration of pseudospins $\{\sigma\}$ with only σ_i flipped. The above equations require $(N + N_\varepsilon) \times 2^N$ basis states to solve, where N is the number of sites and N_ε is the number of energy meshes for the substrate continuum states. It is clear that for $N \sim \mathcal{O}(10)$ the problem becomes formidable.

However, the problem can be projected into a simpler one with an electron at site i and a single pseudospin at site j by taking the summation of both sides of Eqs. (3) and (4) with respect to $\{\bar{\sigma}\}$, where $\{\bar{\sigma}\}$ is the pseudospin configuration except for σ_j , i.e., $|\sigma_j\rangle |\{\bar{\sigma}\}\rangle = |\{\sigma\}\rangle$. The Schrödinger equa-

tions of Eqs. (3) and (4) then become, with new definitions of dynamical coefficients $C_{i\sigma_j}(\tau) \equiv \sum_{\{\bar{\sigma}\}} C_{i\{\sigma\}}(\tau)$ and $C_{\varepsilon\sigma_j}(\tau) \equiv \sum_{\{\bar{\sigma}\}} C_{\varepsilon\{\sigma\}}(\tau)$,

$$i \frac{\partial}{\partial \tau} C_{i\sigma_j}(\tau) = t C_{i+1\sigma_j}(\tau) + t C_{i-1\sigma_j}(\tau) + \frac{\omega_0}{2} [(1 + \sigma_j) + h_i(\tau)] C_{i\sigma_j}(\tau) + g C_{i\sigma_j}(\tau) (1 - \delta_{ij}) + g C_{i(-\sigma_j)}(\tau) \delta_{ij} + \int d\varepsilon T(\varepsilon) C_{\varepsilon\sigma_j}(\tau), \quad (5)$$

$$i \frac{\partial}{\partial \tau} C_{\varepsilon\sigma_j}(\tau) = \frac{\omega_0}{2} [(1 + \sigma_j) + h_\varepsilon(\tau)] C_{\varepsilon\sigma_j}(\tau) + T(\varepsilon) \sum_i C_{i\sigma_j}(\tau) + \varepsilon C_{\varepsilon\sigma_j}(\tau), \quad (6)$$

where the only cost we should pay is an introduction of the molecular fields $h_i(\tau)$ and $h_\varepsilon(\tau)$, which are determined self-consistently at a given τ in terms of $h_i(\tau) = \sum_{l \neq j} \langle 1 + \sigma_l \rangle_i = \sum_{l \neq j} \sum_{\sigma_l} \langle 1 + \sigma_l \rangle_i |C_{i\sigma_l}(\tau)|^2$ and $h_\varepsilon(\tau) = \sum_{l \neq j} \langle 1 + \sigma_l \rangle_\varepsilon = \sum_{l \neq j} \sum_{\sigma_l} \langle 1 + \sigma_l \rangle_\varepsilon |C_{\varepsilon\sigma_l}(\tau)|^2$. The quality or reliability of the approximation introducing the molecular fields will be discussed later. Now the problem can be solved completely by tracking $(N + N_\varepsilon) \times N$ differential equations with each initial condition $C_{i_0(\sigma_j=-1)}(0) = 1$.

III. PROPAGATION OF POLARIZATION

By way of a coupling between an electron and pseudospins, an electron induces the pseudospin flip. The electron transport by the hopping parameter t further leads to the propagation of pseudospin flip. We study how the pseudospin flip would propagate in the ultrafast time region after an electron-injection depending on electronic and molecular degrees of freedom. In this section, we assume $T(\varepsilon) = 0$.

A. Propagation phase diagram

One can define an interesting and useful quantity $I_j(\tau) = \sum_i |C_{i(\sigma_j=1)}(\tau)|^2$ from a solution of the projected Schrödinger equation [Eqs. (5) and (6)], which shows the propagation of pseudospin flip by summing out the electron motion. Figure 1 shows the propagation of pseudospin flip for a fixed value of $\tilde{g} = g/t = 1.6$. The calculation has been done for a molecular array with $N = 201$ sites ($-100 \leq i, j \leq 100$). The designated position for an initial electron-injection is $i = i_0 = 0$. All the quantities in the figure are scaled and redefined by the electron hopping parameter t ($\tilde{\omega}_0 = \omega_0/t$ and $\tilde{\tau} = \tau$). It is in fact found that an entire process occurs in the ultrafast time range, actually in the femtosecond range, by noting that $\delta\tilde{\tau} = 1$ corresponds to 0.66 fs for $t = 1$ eV, 6.6 fs for $t = 0.1$ eV, and the like.

As illustrated in Fig. 1, we find at least three qualitatively different behaviors of propagation of pseudospin flip. It is interesting to examine the motion of center of gravity of the pseudospin flip profile with respect to time in order to understand the nature of propagation. According to Fig. 2, for two extreme cases of small $\tilde{\omega}_0$ ($=0.06$) and large $\tilde{\omega}_0$ ($=4.8$), their

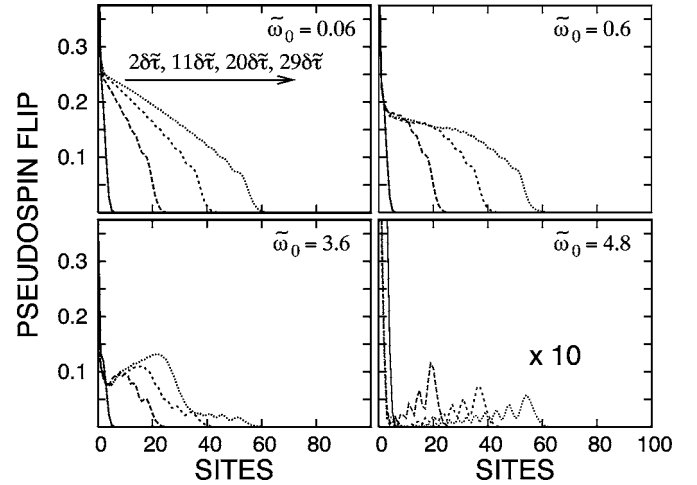


FIG. 1. Snapshots of propagation of pseudospin flip $[I_j(\tau)$ at site $j]$ with respect to values of $\tilde{\omega}_0$ for a fixed $\tilde{g} = 1.6$. Snapshots are taken at $\tilde{\tau} = 2\delta\tilde{\tau}$, $11\delta\tilde{\tau}$, $20\delta\tilde{\tau}$, and $29\delta\tilde{\tau}$, where $\delta\tilde{\tau} = 1$. The quantity $I_j(\tau)$ designating pseudospin flip is a dimensionless number between 0 and 1.

centers of gravity move linearly with $\tilde{\tau}$, but, for a case of an intermediate value of $\tilde{\omega}_0$ ($=3.6$), its center of gravity follows $\sqrt{\tilde{\tau}}$. A similarity between two extreme cases in the former can be easily understood. For both cases, an electron is expected to move like a bare electron because there is little energy cost in an excitation of pseudospin flip for small $\tilde{\omega}_0$, while an excitation is almost forbidden for large $\tilde{\omega}_0$. Thus it is noted that for large $\tilde{\omega}_0$, the pseudospin flip is suppressed by an order of magnitude compared to the other case. For an intermediate value of $\tilde{\omega}_0$, an electron moves in a complicated way, strongly coupled with pseudospins. We can characterize the linear temporal behavior as “ballistic (B)” and, to distinguish behaviors between small and large $\tilde{\omega}_0$, we call them “ballistic first kind (B₁)” and “ballistic second kind (B₂),” respectively. In the same way, the square-root temporal behavior can be characterized as “diffusive (D).” In the inset of Fig. 2, we give a sketch of the propagation phase diagram. The phase boundary is not sharp.

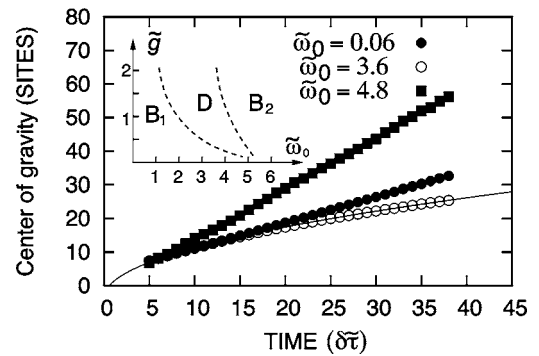


FIG. 2. Motion of centers of gravity of the pseudospin flip profiles with respect to time. A thin solid line is a fitting from $\propto \sqrt{\tilde{\tau}}$ for $\tilde{\omega}_0 = 3.6$. $\tilde{g} = 1.6$ is used. The inset shows a sketch of the propagation phase diagram.

B. Ballistic and diffusive propagation

To understand the ballistic propagation, a previous study on the propagation of 1D Frenkel exciton is useful.¹⁷ In the study, the explicit time-dependent propagation of a single electron (or exciton) wave function $|\Psi(\tau)\rangle$ is examined based on a simple Hamiltonian,

$$\mathcal{H} = t \sum_i (c_i^\dagger c_{i+1} + c_{i+1}^\dagger c_i).$$

In the system, an electron propagation is described by the time-dependent Schrödinger equation for $|\Psi(\tau)\rangle = \sum_i \alpha_i(\tau) |i\rangle$. This model is simple enough to allow an analytic approach. By defining the lattice Green's function as $|\Psi(\tau)\rangle = G(\tau) |\Psi(0)\rangle$ and noting its property from the translational symmetry $G_{i-j}(\tau) = \langle i | G(\tau) | j \rangle$, then $|\alpha_i(\tau)|^2 = |G_i(\tau)|^2$ is readily obtained from $\alpha_i(\tau) = \sum_j G_{i-j}(\tau) \alpha_j(0)$ with $\alpha_j(0) = \delta_{j0}$, i.e., $j=0$ is a starting point. $G_i(\tau)$ is evaluated from a generating function $F(\tau, z)$ defined by

$$F(\tau, z) = \sum_i G_i(\tau) z^i.$$

From the Schrödinger equation, $F(\tau, z)$ can be integrated into $F(\tau, z) = \exp[-i\tilde{\tau}(z+z^{-1})]$ and $|G_i(\tau)|^2$ is then immediately found to be

$$|G_i(\tau)|^2 = J_i^2(2\tilde{\tau}) = \rho_i(\tau) = |\alpha_i(\tau)|^2,$$

where $\rho_i(\tau)$ is interpreted as the probability of finding an electron at site i and $\sum_i |\rho_i(\tau)|^2 = 1$ is also confirmed. $J_i(x)$ is the Bessel function of the order i . The motion of the center of gravity of the system is found to follow $\langle i^2 \rangle = \sum_i i^2 |\alpha_i(\tau)|^2 \propto \tau^2$, i.e., $\sqrt{\langle i^2 \rangle} \propto \tau$.

Two kinds of ballistic propagation of pseudospin flips (B₁ and B₂) can now be understood from the electron density $\rho_i(\tau)$ of the above simple model because an electron moves like a bare electron in both cases. In the region of B₁, the energy cost in order to excite a single pseudospin flip is so small that the kinetic energy of an electron is almost conserved with indefinitely many flips. In this case, flipped pseudospins would not tend to restore to unflipped states. Therefore, the propagation shown in Fig. 1 ($\tilde{\omega}_0=0.06$) can be approximated by integrating $\rho_i(\tau)$ up to a fixed time $\tilde{\tau}$, i.e., $I_i(\tau) \propto \int_0^{\tilde{\tau}} d\tilde{\tau}' J_i^2(2\tilde{\tau}')$. On the other hand, in another ballistic region (B₂), the energy cost for a pseudospin flip is so high that only a tiny fixed amount of flip is available, which also almost conserves the kinetic energy of an electron. Pseudospin flip propagation is then directly proportional to electron density, i.e., $I_i(\tau) \propto J_i^2(2\tilde{\tau})$. In the left panel of Fig. 3, a direct comparison between our full calculations of $\tilde{\omega}_0=0.06$ and $\tilde{\omega}_0=4.8$ and the results of an analytic model is shown. Once we are away from an electron-injection point, nice agreements are obtained. Those agreements guarantee, in a self-evident way, the reliability of the approximation with molecular fields $h_i(\tau)$ and $h_e(\tau)$ introduced in Sec. II.

Diffusive propagation in the region of D is not so simply understood because of the strong coupling of an electron and pseudospins. Instead, in the region, we can explicitly observe the formation of a polaron from a bare electron. In the right

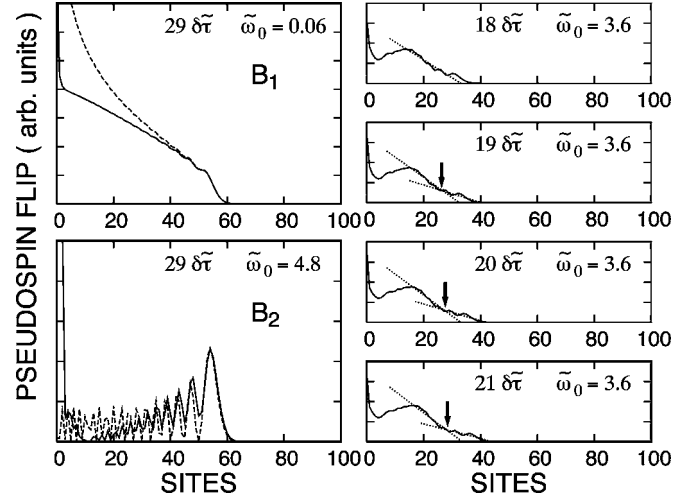


FIG. 3. Ballistic and diffusive propagation. In the left panel, the solid lines are full calculations (shown in Fig. 1; $\tilde{g}=1.6$) and the dashed lines are from a simple analytic model (Ref. 17) for both B₁ ($\tilde{\omega}_0=0.06$) and B₂ ($\tilde{\omega}_0=4.8$). For B₁, a full calculation is compared with $\int_0^{\tilde{\tau}} d\tilde{\tau}' J_i^2(2\tilde{\tau}')$ and, for B₂, with $J_i^2(2\tilde{\tau})$, where $J_i(x)$ is the Bessel function of the order i . In the right panel, an onset of separation (see arrows) of pseudospin flip into dominant part and tail is illustrated for the case of diffusive propagation (D). The dotted lines are guides for the eye. The unit taken in each figure is arbitrary. Only a comparison of shapes is meaningful.

panel of Fig. 3, the propagation is illustrated from $\tilde{\tau}=18\delta\tilde{\tau}$ to $\tilde{\tau}=21\delta\tilde{\tau}$. At $\tilde{\tau}=21\delta\tilde{\tau}$, one can clearly observe the separation of the pseudospin flip into the dominant part and the tail. The onset is presumed to be around $\tilde{\tau}=19\delta\tilde{\tau}$ and would signify the formation of a polaron. As seen in Fig. 1, an end of tail of D ($\tilde{\omega}_0=3.6$) arrives as far as the front edge of pseudospin flips of B₁ ($\tilde{\omega}_0=0.06$ or 0.6) and B₂ ($\tilde{\omega}_0=4.8$) at a given time $\tilde{\tau}$. However, as time goes on, the dominant part is more and more retarded with respect to the tail. Therefore, we naturally claim that the tail part should be from a bare electron, while the retarded dominant part be from a polaron. The retardation of a polaron is attributed to its massive property.

IV. TUNNELING OF AN ELECTRON INTO A SUBSTRATE

In an actual situation, a moving electron at the interface would be captured through tunneling into a substrate. Such a capturing process can be considered in our study through $T(\varepsilon)$. In the study, we take $T(\varepsilon)$ simply as a constant, that is, $T(\varepsilon)=\mathcal{T}$. When \mathcal{T} is an infinitesimal number η ($\eta \rightarrow 0$), we find

$$\Delta I_j(\tau) \equiv [I_j(\tau; 0) - I_j(\tau; \eta)] \propto \eta^2, \tag{7}$$

where $I_j(\tau; \eta)$ has an extended definition compared to $I_j(\tau)$ in the previous section, with $\mathcal{T}=\eta$, $I_j(\tau; \eta) = \sum_i |C_{i(\sigma_j=1)}(\tau)|^2 + \int d\varepsilon |C_{\varepsilon(\sigma_j=1)}(\tau)|^2$. Up to the second order of a finite \mathcal{T} , $I_j(\tau; \mathcal{T})$ can then be expressed as, in terms of $\Delta I_j(\tau)$,

$$I_j(\tau; \mathcal{T}) = I_j(\tau; 0) - \frac{\mathcal{T}^2}{\eta^2} \Delta I_j(\tau). \tag{8}$$

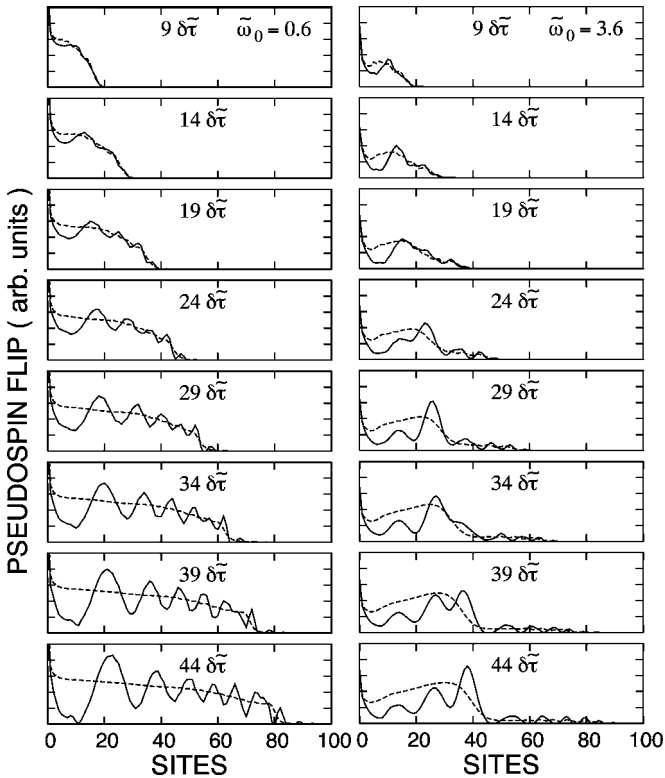


FIG. 4. Effects of an electron tunneling into a substrate on the pseudospin flip with respect to time. $\tilde{g}=1.6$ is used. Left panel: $\tilde{\omega}_0=0.6$. Right panel: $\tilde{\omega}_0=3.6$. The solid lines are calculations with $T/\sqrt{t}=0.04$, but the dashed lines are with $T=0$.

In Fig. 4, we show the propagation of pseudospin flip when accounting for an electron capture by a substrate for $\tilde{\omega}_0=0.6$ (B₁) and $\tilde{\omega}_0=3.6$ (D) up to the second order of \mathcal{T} . For larger values of $\tilde{\omega}_0$, i.e., for B₂, as discussed previously, the pseudospin flip is strongly suppressed even without a capturing process. Effects of an electron capture are different depending on values of $\tilde{\omega}_0$. But, in both cases, the pseudospin at the site that an electron has just passed flips to +1 and tends to restore to -1 as time elapses. For $\tilde{\omega}_0=0.6$ in the left panel of Fig. 4, at the sites near an electron-injection point (i_0 , i.e., $i_0=0$) where a relatively long time has elapsed after an electron passed, pseudospins tend to rapidly precipitate to unflipped states with respect to time. On the other hand, for $\tilde{\omega}_0=3.6$ in the right panel, pseudospins at the same sites partly restore to -1, but a finite amount of pseudospin flip is found to be robust with time.

It is interesting to consider the problem of controlling an array of pseudospin flip. One can possibly produce an array of pseudospin flip in a controlled fashion by controlling the electron hopping parameter t , which is adjusted by the kinetic energy of an injected electron. The case of B₁ may be useful to obtain an array of uniform pseudospin flip. However, we find that the maximum length of the uniform array exists for a strong electron capture, that is, for a large value of \mathcal{T} . In other words, for the left panel of Fig. 4, the maximum length of the approximately uniform array for a given value of \mathcal{T} ($\mathcal{T}/\sqrt{t}=0.04$)¹⁸ would be $\lesssim 55$ sites. If one tries to let propagation continue beyond ~ 55 sites, one would sig-

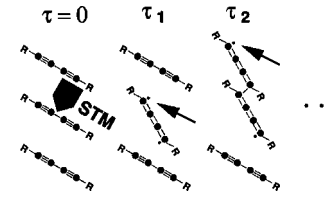


FIG. 5. Excitation of diradicals and spontaneous polymerization of 10,12-pentacosadiynoic acid molecules triggered by STM. Arrows indicate a moving radical with an unbonded electron (dot). In the figure, the closed circle signifies the carbon atom and “R” the substituent. We have $0 < \tau_1 < \tau_2$.

nificantly lose the pseudospin flip at sites near an electron-injection point. On the other hand, the case of D, as shown in the right panel of Fig. 4, can be useful to get a long array of pseudospin flip, but the flips are not uniform along an array. The probability of flipping is highest near the front edge of propagation (polaronic propagation) and decreases as an electron-injection point is approached.

V. DISCUSSION AND CONCLUSION

The physics of extra electrons (or excitons) at the interface of molecular adlayer on substrate matrices is not only of scientific interest but also of practical importance, especially in nanoscale fabrication for molecular electrochemistry. The present model discussed in this paper can be applied to the STM-induced polymerization of diacetylene compounds on a graphite surface by Okawa and Aono.⁷ They succeeded in inducing and controlling the spontaneous chain polymerization, i.e., initiating and terminating at any chosen point. For such nanoscopic control of polymerization, they created an artificial defect in advance with a STM tip. In the STM-induced polymerization by Okawa and Aono, we point out that it is a radical with an unbonded electron that hops among molecules, as depicted in Fig. 5. Our original model can be applied as it is to the diacetylene polymerization by noting that a moving radical can be taken as a Frenkel exciton in a mathematical sense. Then the molecular polarization in our model (ω_0 described by pseudospins σ_{i+} and σ_{i-}) should be an excitation to the lowest $\pi\pi^*$ triplet state of a diradical of 10,12-pentacosadiynoic acid molecules with $\omega_0 = 3.1$ eV. In the experiment, it is also found that the spontaneous polymerization persists up to thousand sites, which implies that the value of \mathcal{T} taken for demonstration in Fig. 4 is rather on the large side.¹⁸ Our description would provide another possible mechanism for the phenomena which does not require thermal fluctuation. In contrast, in the mechanism suggested by Okawa and Aono, once a diradical is excited, thermal vibration triggers an additional reaction forming a dimer of diacetylene.^{19,20} Therefore, it could be a good candidate for experiments in order to elucidate which mechanism is correct to measure the propagation rate. A reaction by the present mechanism could occur orders of magnitude more rapidly than the thermal fluctuation mechanism.²¹

Let us summarize the work. We have proposed a model of a single local excitation and molecules on the 1D molecular array, where molecules are approximated to have two levels,

that is, a ground state and a polarized state. A local excitation can be an electron wave packet or an exciton introduced by an external perturbation. Within such a framework, we studied the dynamics of an electron (or exciton) and its accompanying propagation of molecular polarizations. Depending on the system parameters like ω_0/t ($=\tilde{\omega}_0$) and g/t ($=\tilde{g}$), we found there are three distinct possible propagation phases—two kinds of ballistic propagation (B_1 and B_2) and one diffusive propagation (D). Ballistic propagation can be well understood from an analytic model of the 1D Frenkel exciton (in fact, a bare electron or bare exciton in our case). Incidentally, diffusive propagation implies the formation of a massive polaron compared to a bare electron. We provided a sketch of the phase diagram. In a realistic situation, moving electrons at the interface would be captured by a substrate, which could be taken into account in the work. In this case,

we discussed possibilities and limitations for controlling an array of polarized molecules. Finally, we discussed recent experiments of STM-induced polymerization of a diacetylene compound (10,12-pentacosadiynoic acid) in relation to our model. We suggest that our model of transport of a local excitation which is coupled with molecular polarizations provide a possible mechanism to explain the experiment.

ACKNOWLEDGMENTS

We appreciate constructive discussions with Masao Arai, Yuji Okawa, and ByungIl Min. This work was supported by Special Coordination Funds for Promoting Science and Technology from the Ministry of Education, Culture, Sports, Science and Technology of the Japanese Government.

-
- ¹N. H. Ge, C. M. Wong, R. L. Lingle, Jr., J. D. McNeill, K. J. Gaffney, and C. B. Harris, *Science* **279**, 202 (1998).
²A. D. Miller, I. Bezel, K. J. Gaffney, S. Garret-Roe, S. H. Liu, P. Szymanski, and C. B. Harris, *Science* **297**, 1163 (2002).
³D. G. Busch, S. Gao, R. A. Pelak, M. F. Booth, and W. Ho, *Phys. Rev. Lett.* **75**, 673 (1995).
⁴S. L. Dexheimer, A. D. Van Pelt, J. A. Brozik, and B. I. Swanson, *Phys. Rev. Lett.* **84**, 4425 (2000).
⁵A. Sugita, T. Saito, H. Kano, M. Yamashita, and T. Kobayashi, *Phys. Rev. Lett.* **86**, 2158 (2001).
⁶S. A. Trugman, L. Ku, and J. Bonca, *J. Supercond.* **17**, 193 (2004).
⁷Y. Okawa and M. Aono, *Nature (London)* **409**, 683 (2001).
⁸M. Akai-Kasaya, K. Shimizu, Y. Watanabe, A. Saito, M. Aono, and Y. Kuwahara, *Phys. Rev. Lett.* **91**, 255501 (2003).
⁹J. Shah, *Ultrafast spectroscopy of semiconductors and semiconductor nanostructures* (Springer, New York, 1999); *Ultrafast phenomena*, edited by T. Elsaesser, T. Mukamel, M. M. Murnane, and N. F. Scherer (Springer, Berlin, 2001).
¹⁰R. D. Averitt and A. J. Taylor, *J. Phys.: Condens. Matter* **14**, R1357 (2002).
¹¹G. Dujardin, R. E. Walkup, and Ph. Avouris, *Science* **255**, 1232 (1992); B. C. Stipe, M. A. Rezaei, W. Ho, S. Gao, M. Persson, and B. I. Lundqvist, *Phys. Rev. Lett.* **78**, 4410 (1997); and references therein.
¹²N. Nagaosa and T. Ogawa, *Phys. Rev. B* **39**, 4472 (1989); K. Nasu, *Rep. Prog. Phys.* **67**, 1607 (2004); K. Yonemitsu and K. Nasu (unpublished); and references therein.
¹³It corresponds to an extension to the many-body problem from the one-body problem under the time-dependent perturbation by V. Weisskopf and E. Wigner, *Z. Phys.* **63**, 54 (1930).
¹⁴J. D. Lee, O. Gunnarsson, and L. Hedin, *Phys. Rev. B* **60**, 8034 (1999); J. D. Lee, *ibid.* **61**, 8062 (2000).
¹⁵J. D. Lee and M. Nishino, *Phys. Rev. B* **72**, 195111 (2005); J. D. Lee, J. Inoue, and T. Kuroda (unpublished).
¹⁶G. D. Mahan, *Many-particle physics* (Plenum, New York and London, 1986).
¹⁷R. E. Merrifield, *J. Phys. Chem.* **28**, 647 (1958).
¹⁸It should be understood that the value of \mathcal{T} taken in Fig. 4 is more or less exaggerated for demonstration of its effects.
¹⁹W. Neumann and H. Sixl, *Chem. Phys.* **58**, 303 (1981).
²⁰Y. Okawa and M. Aono, *J. Chem. Phys.* **115**, 2317 (2001).
²¹Y. Okawa (private communication).